

AD-A122 799

ANALYSIS OF TRANSONIC WINDTUNNEL FLOWS: BOUNDARY
CONDITIONS FOR PERFORATE... (U) CITY UNIV LONDON
(ENGLAND) DEPT OF AERONAUTICS M M FREESTONE ET AL.

1/1

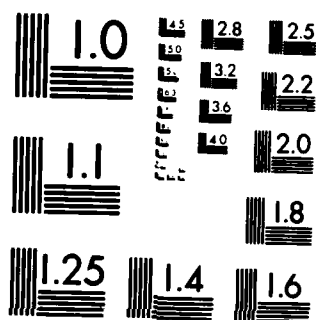
UNCLASSIFIED

22 OCT 82 AERO-82/2 EOARD-TR-83-1

F/G 20/4

NL

END
DATE
FILMED
DTIC



MICROCOPY RESOLUTION TEST CHART
NATIONAL BUREAU OF STANDARDS-1963-A

ADA122799

THE CITY UNIVERSITY

(2)

ANALYSIS OF TRANSONIC WINDTUNNEL FLOWS:
BOUNDARY CONDITIONS FOR PERFORATED WALL
WINDTUNNEL FLOWS.

By
Dr. M.M. Freestone and Dr. P. Henington

DTIC
ELECTE
DEC 28 1983
S H D

Research Memo. Aero 82/2

October 1982.



St. John Street, London, EC1V 4PB Telephone: 01-253 4399

This document has been approved
for public release and sale; its
distribution is unlimited.

FILE COPY

82 12 28 028

Unclassified

REPORT DOCUMENTATION PAGE		READ INSTRUCTIONS BEFORE COMPLETING FORM
1. REPORT NUMBER EDARD-TR-83= 1	2. GOVT ACCESSION NO. AD A122	3. RECIPIENT'S CATALOG NUMBER 799
4. TITLE (and Subtitle) Analysis of Transonic Windtunnel Flows : Boundary Conditions for Perforated Wall Windtunnel Flows		5. TYPE OF REPORT & PERIOD COVERED Final Scientific Report 1 January 1982-31 August 82
		6. PERFORMING ORG. REPORT NUMBER The City University Research Memorandum Aero-82/27
7. AUTHOR(s) M.M. Freestone, P. Henington		8. CONTRACT OR GRANT NUMBER(s) AFOSR 82-0129
9. PERFORMING ORGANIZATION NAME AND ADDRESS The City University Department of Aeronautics Northampton Sq., London ECIV OHB England		10. PROGRAM ELEMENT, PROJECT, TASK AREA & WORK UNIT NUMBERS 61102F PE 2301/D1 Proj/Task
11. CONTROLLING OFFICE NAME AND ADDRESS European Office of Aerospace Research and Development, Box 14, FPO New York 09510		12. REPORT DATE 22nd October 1982
14. MONITORING AGENCY NAME & ADDRESS (if different from Controlling Office) European Office of Aerospace Research and Development, Box 14, FPO New York 09510		13. NUMBER OF PAGES 31
		15. SECURITY CLASS. (of this report) Unclassified
15a. DECLASSIFICATION/DOWNGRADING SCHEDULE		
16. DISTRIBUTION STATEMENT (of this Report) Approved for public release; distribution unlimited		
17. DISTRIBUTION STATEMENT (of the abstract entered in Block 20, if different from Report)		
18. SUPPLEMENTARY NOTES		
19. KEY WORDS (Continue on reverse side if necessary and identify by block number) Transonic, Windtunnel, perforated liner, boundary layers, boundary conditions.		
20. ABSTRACT (Continue on reverse side if necessary and identify by block number) A scheme for obtaining an improved boundary condition relevant to the perforated walls of transonic windtunnels is reviewed and the sources of possible errors involved in its practical application are assessed. Earlier work by the authors to implement the scheme provided measured boundary layer development and flow directions just outside the boundary layer in The City University transonic windtunnel. This work is shown to have been subject to errors from two main sources. First the yawmeter calibrations (cont		

DD FORM 1473
1 JAN 73

EDITION OF 1 NOV 65 IS OBSOLETE

Unclassified

SECURITY CLASSIFICATION OF THIS PAGE (When Data Entered)

20.

→ were not sufficiently accurate, and the remedy for this is presented. Second, lateral nonuniformity was present which produced significant flow angle variations. This nonuniformity is shown to be much reduced by windtunnel alterations, possibly the most important of these being an increase of the open-area ratio of the antiturbulence screens. ←

Unclassified

SECURITY CLASSIFICATION OF THIS PAGE(When Data Entered)

EQAPD-TR-83- 1

This report has been reviewed by the Information Office (EOARD/CI) and is releasable to the National Technical Information Service (NTIS). At NTIS it will be releasable to the general public, including foreign nations.

This technical report has been reviewed and is approved for publication.

William R. Brandt

WILLIAM R. BRANDT
Major, USAF
Chief, Flight Vehicles

FOR THE COMMANDER

Jerry R. Bettis

JERRY R. BETTIS
Lt Colonel, USAF
Deputy Commander

Accession For	
NTIS GRA&I	<input checked="checked" type="checkbox"/>
DTIC TAB	<input type="checkbox"/>
Unannounced	<input type="checkbox"/>
Justification	
By _____	
Distribution/	
Availability Codes	
Dist	Avail and/or Special
A	



ANALYSIS OF TRANSONIC WINDTUNNEL FLOWS :
BOUNDARY CONDITIONS FOR PERFORATED WALL
WINDTUNNEL FLOWS.

By

M.M. FREESTONE AND P. HENINGTON

Research Memo. Aero 82/2

October, 1982

Abstract :

A scheme for obtaining an improved boundary condition relevant to the perforated walls of transonic windtunnels is reviewed and the sources of possible errors involved in its practical application are assessed. Earlier work by the authors to implement the scheme provided measured boundary layer development and flow directions just outside the boundary layer in The City University transonic windtunnel. This work is shown to have been subject to errors from two main sources. First the yawmeter calibrations were not sufficiently accurate, and the remedy for this is presented. Second, lateral nonuniformity was present which produced significant flow angle variations. This nonuniformity is shown to be much reduced by windtunnel alterations, possibly the most important of these being an increase of the open-area ratio of the antiturbulence screens.

1. INTRODUCTION

It has been recognized for several years (e.g. Ref.1) that if the effects of the wall liners of a ventilated transonic windtunnel are to be accurately represented in a computational scheme, for example in one such as that due to Catherall (Ref.2), then a simple linear boundary condition such as

$$\phi_x \pm F \phi_{xz} \pm \frac{1}{P} \phi_z = 0, \quad (1)$$

where F, P are taken to be constant for a given wall geometry and flow Mach number, is quite inadequate. (For fuller details of eqn.(1), see Refs 2 and 3)

In the case of windtunnels with slotted liners, Berndt and Sorensen (Ref.4) have addressed the problem of improving on eqn.(1), and work is continuing on this. (Ref.5). For perforated walls, to which our investigations are limited, and for wind speeds in the high subsonic range, the possibility of properly incorporating the influences of boundary layer growth, as well as flow transpiring through the liner perforations, has been explored by Chan (Ref.6) and the present authors. (Refs. 7, 8, 9). The present authors have described a flow model consisting of two interacting elements, namely the wall liner boundary layer and the quantitative mass transfer through the liner perforations. They have made a preliminary assessment of the accuracy of this flow model for predicting wall flows measured in the perforated liner transonic windtunnel of The City University. The present work, supported by a grant from the USAF*, is concerned mainly with making improvements in the accuracy of predictions given by the method for supposedly two-dimensional windtunnel flows. All the experiments to be described have been conducted in the transonic windtunnel of The City University, and descriptions of this windtunnel appear in Refs. 7 and 9.

In order to make the present report reasonably self-contained a brief exposition of the ideas on which the flow model is based is next presented. This is followed by a discussion of the accuracy yielded by the method as assessed at the commencement of the grant period, and then a description of the work aimed at improving on this accuracy.

(Footnote * - Grant Number AFOSR 82-0129)

2. Description of the Flow Model Capable of Yielding a Perforated Wall Boundary Condition.

If a way can be provided of linking the local pressure to the flow direction at each point in the inviscid flow close to the windtunnel liners then a suitable wall boundary condition may be obtained. To provide such a link an idealized model of the two-dimensional windtunnel test situation is introduced for the flow near the perforated wall liners. First it is supposed that the boundary layer of the flow passing close to each liner reacts like a transpiring boundary layer with fluid entering or leaving the working section via the plenum chambers. The boundary layer is generally subjected to variations in transpiration rate as it progresses along the working section. Generally where there is locally low pressure (i.e. pressure on the flow side of the liner is lower than plenum chamber pressure) the boundary layer will be "blown" and will tend to grow rather rapidly, and conversely high local pressure will give "suction" and a thinning of the boundary layer. Part of our model then is to construct a prediction method that will adequately yield the boundary layer behaviour on a perforated liner with specified transpiration rates. It is not necessary to predict the detailed boundary layer parameters, but only integral properties such as δ^* and H .

Thus the boundary layer element of the model has to yield δ^* , H for given initial (i.e. upstream) values of δ^* and H ; given reference Reynolds number and Mach number, and given variations of local mass transfer parameter $\theta_w = \frac{\rho_w \phi_w}{\rho_e U_e}$, and flow speed U_e . † We may assume that streamwise variations in Mach number are not significant in directly influencing the boundary layer by compressibility changes although the boundary layer will react to streamwise pressure gradient variations in addition to changes in transpiration rate as a result of θ_w varying. Up to the present we have made use of an adaptation (Ref.9) of the entrainment method (Ref.10) for this boundary layer prediction. It might at some stage be necessary to improve on this method. Chan (Ref.11) has produced a mixing length method which could possibly be used as an alternative.

† The notation follows that of Ref.8, throughout.

The second element of the flow model is the representation yielding the values of the mass transfer parameter, θ_w , itself. We postulate that the local wall flow environment will effectively define local values of θ_w , and this parameter cannot be influenced by distant events other than through the way they change the local environment. This local environment we see as needing several parameters for its specification. These are

(a) Local liner geometry, for example, perforation diameter and inclination, plate thickness, and open area ratio.

(b) Local pressure difference across the liner,

$$\Delta p = p_w - p_{pl}$$

(c) Local dynamic pressure at the edge of the boundary layer (or a short distance beyond), q_e .

(d) Local Mach number just outside the boundary layer, M_e .

(e) Local boundary layer parameters, δ^* , shape factor, and so on

(f) Local Reynolds number R_{δ^*}

We adopt a simple form of specification, which for a given wall geometry may be written in functional form as

$$f \left(\frac{\Delta p}{q_e}, \theta_w, M_e, \delta^* \right) = 0. \quad (2)$$

Whereas it is possible that the other parameters have a significant influence we shall disregard them unless and until it proves necessary to do otherwise.

It was judged earlier that the only way of determining the functional form (2) would be from carefully conducted windtunnel experiments. No theoretical model of the flow currently envisaged could yield sufficiently accurate results. It is by no means clear how experiments should best be conducted to yield the dependence (2). As detailed in Ref.8 the method we have adopted is indirect and entails measuring streamwise (i.e. x-wise) variations of parameters yielding

$$p_w(x), \quad p_{p1}(x), \quad \delta^*(x), \quad \frac{v_e}{U_e}(x)$$

along a perforated wall liner.

Since, at the subsonic speeds of interest one may assume the inviscid flow outside the boundary layer is also isentropic, one may deduce from the above distributions the parameters

$$q_e(x), \quad U_e(x), \quad M_e(x), \quad \rho_e(x), \quad \frac{\Delta p}{q_e}(x)$$

Now the equation (Ref.8) relating mass balance through the wall boundary layer yields, for two dimensional flow,

$$\frac{d}{dx} \left\{ \rho_e U_e (L - \delta^*) \right\} + \rho_e v_e - \rho_w v_w = 0. \quad (3)$$

Here conditions "e", referring to "edge of the boundary layer" are taken to be on a plane a distance L from the wall plane. This may be the distance from the wall of a flow angle probe, which when traversed streamwise provides $v_e/U_e(x)$. Thus equation (2) is re-written in the following way so that only measured quantities and quantities directly deduced from measurements appear on the right hand side

$$\frac{\rho_w v_w}{\rho_e U_e} = \frac{\rho_e v_e}{\rho_e U_e} + \frac{1}{\rho_e U_e} \frac{d}{dx} \left\{ \rho_e U_e (L - \delta^*) \right\}$$

The transpiration parameter $\theta_w = \rho_w v_w / \rho_e U_e$ is thus found by substituting observed values on the right. Since differentiation is to be performed, experimental accuracy is exceptionally important in obtaining $\rho_e U_e$ and δ^* .

In Ref.8 it is shown that these two elements may be used in combination to provide a wall boundary condition which represents the effects of the particular type of perforated wall on the inviscid "core" flow through the windtunnel. Since the data for the mass transfer element are obtained experimentally they are indeed specific to the particular windtunnel used. In principle however these experiments may be performed with any perforated wall windtunnel and once done they provide the data needed to represent the boundary condition of that windtunnel.

3. Application of the Method

As has been stated, the objective is to provide an effective inviscid flow boundary condition to represent the wall effects of perforated liners. We have outlined the two elements of boundary layer development and mass transfer. Ref.9 gives details of a possible computational scheme for matching the boundary condition with a finite difference aerofoil flow computation.

However it is not essential to go to this stage to check the effectiveness of the method. One can simply provide a measured perforated wall pressure distribution, and obtain from the method predictions of the boundary layer development and the distribution of the normal velocity component in the inviscid flow near the wall. These predictions may be compared with observations, and the accuracy assessed. This was done earlier (Ref.8) and the comparisons were encouraging, but it was clear that further work was needed to improve the accuracy of the predictions. The relevant figure relating to the predictions from Ref. 8 is reproduced as fig.1. It was aimed to carry out the work necessary for improving the predictions during the grant period. One might conjecture that the accuracy required for $\theta_e = \frac{\rho_e v_e}{\rho_e U_e}$ would be about ± 0.1 deg to ± 0.2 deg, with the former figure being desired *. Some of the values of θ_w are in error by more than this, (fig.1) so one concluded that achievable accuracies for θ_e were probably inadequate.

4. Assessment of the sources of errors

There are numerous sources of errors in all experimental (and theoretical) work. The present method combines both experimental and theoretical data and it is helpful next to list the possible sources of errors relating to the prediction of flow parameters together with comments.

* Our own investigations to assess the degree of accuracy likely to be necessary have so far not proved fruitful.

4.1 Errors in conceptual representation of the flow near and through the wall.

4.1.1 The flow over the wall is not a transpiring boundary layer flow, since the perforations are not negligible in size compared with the boundary layer thickness, nor are they extremely densely spaced over the liner plate surface. (See Ref.9 for details of the windtunnel geometry*) Assuming a boundary layer flow consequently entails approximation.

4.1.2 The mass transfer parameter, although surely capable of being represented in terms of the local flow environment and local pressures is in fact represented by a simplified set of such parameters.

4.2 Errors in obtaining data for the two flow elements

4.2.1 The boundary layer is predicted by a simple integral method which might not be very accurate, particularly since at present there are no effects of compressibility included, nor of surface roughness.

4.2.2 The mass transfer data are obtained by an indirect experimental method which entails measurements of several parameters and also subsequent analysis. Both stages may bring in errors. The main measurements are as follows.

(i) Wall surface pressures

These are subject to error due to imperfect manufacture of tappings, and also with mass transfer occurring there are local pressure fields around each individual perforation giving rise to variations at a tapping location away from the general mean level of pressure defined as an average over a cycle of the perforation pattern. In addition when the boundary layer probe used in our tests (see fig.2) is present it influences the pressures on the walls.

* The wall perforations comprise holes drilled at 60° to the liner normal. Total hole cross section area is 6 percent of the liner wetted area.

(ii) Boundary layer profile

The boundary layer rake of pitot tubes was designed to give only a small disturbance to the upstream pressure field and the upstream flow directions. Consequent errors in determining boundary layer thickness should be small but they might not be negligible. Errors due to assumptions concerning air temperature needed to determine density and speed from pressure are almost certainly negligible.

(iii) Flow angle

Flow angle is found at two different heights above the perforated liner from two Conrad type "yawmeters", see fig.3. To do this requires accurate pressure recording for each meter of the two static pressures on the ground inclined faces (yielding Δp) and a determination of the dynamic pressure, q , in the approaching flow local to the meter. A calibration in the form

$$\theta = m \frac{\Delta p}{q} + c \quad (5)$$

then gives θ , the inclination of the approaching flow relative to a datum line on the yawmeter. Both m and c need to be found from calibration and they are weak functions of the Mach number of the flow in the locality of the yawmeter.

It was relatively easy to find m with sufficient accuracy (see Ref.9). This was not so for c ; and the method originally adopted of evaluating this was an indirect one whereby the absolute flow direction was assumed to be parallel to the boundary layer displacement surface. This method was found to give a standard deviation error for θ of 0.23 degree - a disappointingly poor result.

Analysis of the experimental data to give the mass transfer parameter introduces further uncertainty primarily because of the need to estimate $d\delta^*/dx$. It was believed that

the main source of error here would come from the real boundary layer growth not being precisely two-dimensional. The likely magnitudes of these errors are difficult to estimate. Naturally, the nearer to the two-dimensional conditions the observations prove to be, the better.

4.3 Errors in obtaining effectively two-dimensional pressures and flow directions.

As well as influencing the accuracy of the determination of the data for the mass transfer element, departure from two dimensionality in the wall flow will also affect the comparison of predicted and measured flows. Consequently even if the data were correctly found and the predictions were then applied to situations which were significantly affected by three dimensional boundary layers we should find discrepancies between predicted and observed flow directions and boundary layer thicknesses.

5. Programme of Work aimed at Improving Predictions Accuracy

5.1 Yawmeter Calibration

The foregoing consideration of errors leads one to attempt first of all to improve the accuracy of determining the intercept c (eq 5). We had to devise a new method which would not be dependent on assessing the flow direction indirectly through assuming that local streamlines are parallel to the solid liner boundary layer displacement surface. To remove this dependence it was decided to revert to the standard approach to calibrating yawmeters, which is to present each yawmeter at a specific point in a flow on two different occasions; in the first in its upright orientation, and secondly precisely inverted. When no change in $\Delta p/q$ is noted on inverting the probe one knows that in this orientation the yawmeter axis of rotation is parallel to the local flow.

Although basically a simple concept it was nevertheless very complicated to apply for the two yawmeters attached to the boundary layer probe. It was not possible to de-mount the yawmeters from the probe assembly and the re-mount them so they had to be calibrated whilst attached to the probe (see fig.2). A new probe mount was made which allowed the tip of each yawmeter to be presented upright and inverted as required. However the parts of the probe other than the yawmeter of interest obviously are in different positions in the windtunnel in the upright and inverted situations. Clearly then the flow is likely to be directed slightly differently in the two situations, and it was found to be very important to assess this flow change and to allow for it in the calibration.

Details of the yawmeter calibration runs and the corrections are given in Appendix 1. It is concluded there that the new yawmeter calibration enables flow angle to be measured with a standard deviation of error of 0.045 degree. This compares with the previous calibration procedure which yielded 0.23 degree for the standard deviation of error. This improvement was clearly well worthwhile.

5.2 Lack of Two-Dimensionality of the Windtunnel Boundary Flow

Having achieved a reliable calibration for each of the two yawmeters attached to the boundary flow probe it was disturbing then to find that the flow directions provided by them were different by almost 1 degree. (fig.4) Although related to different heights from the perforated surface this accounted for only a fraction of the observed direction differences. The two yawmeters are displaced laterally from the pitot probe plane of the rake, one to the port by 27.8 mm, the other to the starboard by 27.8 mm. It was concluded that this difference in spanwise location of 55.6 mm must have caused the observed flow direction variation, and the subsequent conclusion was that the flow field in the windtunnel was quite significantly

different from two dimensional conditions. Although it was tempting immediately to try to determine the cause of the spanwise flow nonuniformity it was thought that some further investigation of the flow as it existed would be valuable. The reason for this was that it was thought that the lateral non-uniformities might well be capable of being averaged to yield quite accurate results for possible two dimensional flows. A detailed account of the investigation of the non-uniformity is given in Appendix 2.

6. Improvement of Windtunnel Flow

As mentioned in Appendix 2, the degree of lateral non-uniformity in the wall boundary layer of the City University transonic windtunnel was found to be such that improvements were called for before any further check could be made on the accuracy of the overall wall flow prediction method.

It was realised that there was not sufficient time in the grant period to investigate the source or sources of nonuniformity, to improve the windtunnel if possible, and then to run more tests to check the prediction method. The nature of the investigation and improvement of the windtunnel flow was highly speculative since virtually nothing is available in the literature concerning uniformity of transonic windtunnel liner boundary layers. With flows entering the working section through a contraction cone, having passed through corner vanes and turbulence screens, it could be that considerable non-uniformity is quite common. However it was clear that attention should be given to details of the windtunnel condition and cleanliness. The windtunnel is built in sections, and it was relatively easy to dismantle parts of it to achieve access to the contraction cone, the corner vanes upstream of the contraction and the two gauze screens sited upstream and downstream of these corner vanes. The screens were rather dirty and it was ascertained by measurement that when clean they had open area ratios, β , of 0.49 for the upstream one and 0.405 for the downstream one. In an article on low speed windtunnel

design, Bradshaw and Pankhurst (Ref.12) stated that for values of β less than 0.57 the flow through turbulence screens would form coalescing jets on the downstream side. These would occur in a random but steady pattern and result in small variations in flow direction in the working section, and these in turn would give spanwise variations of boundary layer thickness and shear stress, of the order of ten percent of the mean, in nominally two dimensional boundary layers. Since one may expect the subsonic flow through a perforated wall transonic windtunnel to be qualitatively similar to that of a low speed windtunnel there was a clear indication that the gauzes should be changed. New gauze was purchased and fitted at the end of July 1982. The new gauze had a value of β of 0.57. Other alterations made included tidying up one of the contraction panels, and making good the joints between the windtunnel sections on re-assembly.

In order to make a rapid assessment of boundary layer non-uniformity a spanwise row of twelve Preston tubes was attached to the floor of the working section near its upstream end. Pressure measurements were made using the tubes both before and after the time that the windtunnel alterations were introduced. It had been found that the Preston tube pressures were fairly sensitive to boundary layer thickness change, and therefore they provided a simple and effective way of assessing the changes produced by the alterations. Results of these tests are shown in fig.5, and it is seen that a substantial improvement had been produced. It was felt worthwhile to proceed then to undertake a more complete investigation of the boundary layer both laterally across the floor of the working section and longitudinally. Such boundary layer data together with flow direction data should provide variations in wall flow parameters relating to nearly two dimensional conditions, and should therefore yield results that ought to be predicted reliably by the proposed new boundary condition procedure. Some of these data have already been determined and are presented in fig. 6. However it has not proved possible in the allotted time to make a prediction so that there is no conclusion on the question of whether the

overall accuracy of the prediction method is now adequate or not. Despite this it should prove possible to pursue this question in the near future and report on the results.

7. Conclusions

7.1 Work carried out during the grant period was aimed at improving the demonstrable prediction accuracy of the authors' method for specifying the wall boundary condition applicable to perforated windtunnel liners.

7.2 It was found that the earlier calibration of the yawmeters which are used to provide essential flow direction data for the method, could be considerably improved by reverting to a more commonly used procedure. It was found necessary to account for changes in flow direction (and speed) induced by the probe assembly in order to achieve the desired accuracy in these calibrations. With such corrections incorporated it was determined that the standard deviation of error in the measured flow direction was 0.045 degree.

7.3 With accurate measurements of the wall flow directions available, via the new calibrations, it was discovered that lateral flow direction variations of up to 1 degree were present in the University's transonic windtunnel.

7.4 The non-uniformities were investigated and found to be much reduced by introducing certain alterations to the windtunnel, possibly the most significant of these being the change of the turbulence screens so as to increase their open area ratio.

7.5 It was not possible in the grant period to make an overall re-assessment of the accuracy of the method to see whether it is adequate for its intended use, but work is due to continue on this, and results will be reported when they become available.

Appendix 1
The New Yawmeter Calibrations

A probe mount was designed to allow the tip of each yawmeter to be presented, upright and inverted at the same point in the working section.

Experiments were carried out with both walls perforated, Schlieren was used, and the rake probe placed near to the rear of the working section. The yawmeters were presented upright and inverted at the same position in the flow. i.e. each of the two yawmeters had its own particular position. Thus there were four groups of runs, each group consisting of nine runs. The nine runs included three repeat runs at each of three local Mach numbers, 0.88, 0.76 and 0.68.

The static pressures measured with the rake static tube are corrected* to the yawmeter tip positions. Then a correction** effectively for run Mach number is applied to all pressures used. Then the parameter $\frac{\Delta p}{q}$ is evaluated for each yawmeter, where Δp is the pressure difference between the two yawmeter orifices, and q is the dynamic pressure local to the yawmeter.

Using yawmeter calibration gradients established in Ref.9, it was possible to establish the intercept C of the yawmeter calibration by plotting together the new data obtained in the upright and inverted positions. Corrections* were made for this intercept to account for the flow disturbance, generated by the rake and support during the new experiments. This disturbance is different from that experienced with the rake in normal use against the wall. These corrections were between 0.1° and 0.15° , and were thus considered worthy of application.

*The corrections were calculated using linearized compressible potential theory. All components of the rake and its immediate supporting mechanism were modelled using point sources (for longitudinal tubes) or source lines (to represent tubes yawed in the flow, or plate edges, as required).

The solution of the potential equation was obtained by scaling the lateral dimension by the Prandtl-Glauert factor ($\beta = \sqrt{1-M^2}$). One value of M_∞ was chosen, namely a value appropriate to the calibration at the highest speed in question, $M_\infty = 0.887$.

**This correction is applied, to remove the main effects of windtunnel flow non-repeatability, - all pressures are corrected to a chosen Mach number.

The values of the calibration intercept obtained were estimated to have a standard deviation of error of 0.034° . In fact the experimental data indicated that for a given Mach number (M_{∞}) a repeatability that was typically better than this was achieved.

There was evidence that the values of the calibration intercept and gradient varied with M_{∞} . A linear variation was assumed, for each yawmeter, when generating the final calibration equation.

It was predicted that, when used, the new yawmeter calibration would be capable of generating flow angles which are correct to a standard deviation of error of 0.045 degrees, i.e. a probable error of 0.031 degrees. This is a marked improvement on the old calibration, where values of the flow angle would only be calculated to a standard deviation of 0.23 degrees.

Appendix 2

Windtunnel Flow Non-uniformity

A2.1 Experimental Investigation of Lateral Non-Uniformity of the Windtunnel Flow

In order to investigate the non-uniformity which appeared to be present in the windtunnel flow, a set of experiments was prescribed and carried out. These experiments consisted of traverses across the bottom wall of the windtunnel with the combined boundary layer and yawmeter rake. The traverses were carried out at two longitudinal positions; 37mm downstream of the beginning (i.e. upstream edge) of the bottom wall liner (but still in the region where the wall is solid) and 240mm downstream of the beginning (where the wall is perforated). At each longitudinal position, two flow configurations were generated. The first, with a freestream Mach number of approximately 0.78, involved suction through the perforated wall and for this configuration, the flow angle outside the boundary layer was of the order of one degree (flow directed towards the wall). The second configuration involved strong blowing through the wall, with flow angles, again outside the boundary layer, of two degrees (away from the wall). Here the free-stream Mach number was lower than earlier at approximately 0.65.

Using the combined boundary layer and yawmeter rake, measurements were made of local static pressure, boundary layer displacement thickness, and flow (pitch) angle outside the boundary layer. The latter angle was measured simultaneously at the two yawmeters, mounted with the rake. In the upstream traverse, measurements were made at seven lateral positions spanning 77mm of the 230mm windtunnel width. In the downstream traverse, only five measuring positions were used, covering 46mm of the windtunnel width. A diagram of the respective rake foot positions on the bottom wall liner is shown in Figure 7.

The procedure adopted for analysing the experimental data, broadly follows that described in Section (4.3.3) of Reference 9. However, the following two departures were made from that approach. First, the pressure field generated by the rake when in the presence of the bottom wall liner has not been modelled. As such, it was not possible to apply

any correction to the pressures measured at the rake static tube to make them exactly appropriate to the yawmeter tips or the boundary layer rake foot. Second, during the rake traverses carried out at the position $X = 240\text{mm}$, the foot of the boundary layer rake was clearly sited in the perforated region of the wall liner. To avoid incorporating the localized effects of individual perforations in the results, the foot was moved always to the same position relative to a cycle of the hole pattern. This caused the longitudinal position of the rake to vary slightly from experiment to experiment. From data presented in Reference 9, it was possible to correct the values of δ for these variations. The distributions of boundary layer displacement thickness across the bottom wall liner are shown in Figure 8.

Static pressures measured using the rake mounted tube in the position $X = 37\text{mm}$, are shown in Figure 10. These have been corrected for the variation in freestream Mach number between experiments. They are presented in non-dimensional form, the denominator being the ambient pressure outside the windtunnel. This choice of denominator is sensible when one considers that we are expecting to discover undesirable variations in the stagnation pressure local to the rake.

Finally, values of the flow angle at the two yawmeter positions are calculated. Again, this is carried out using the original procedure, but now the improved yawmeter calibration, described in Appendix 1, is used. Before the results from the two yawmeters can be compared, it is necessary to account for the change in flow angle between their levels. This can be achieved by use of the continuity equation, provided that the longitudinal pressure gradient near the rake is known. Careful estimates were made of these gradients, from other available pressure data, relevant to the experiments in question. The corrections are applied so as to express the results from the higher of the two yawmeters (Number 2) at the level of the lower one, namely 19.8mm from the wall. These corrections are small, not exceeding 0.25 degree in flow angle. It was mentioned earlier that between some of the experiments, the longitudinal position of the rake varied, as it was moved across the bottom perforated wall, and that corrections for this were applied to values of the boundary layer displacement thickness. Similar changes are made here to values of the flow angle. In Figure 9, the variations

in calculated flow angle across the bottom wall are shown.

A.2.2 Discussion of Results from flow uniformity investigation

In Figure 10 the variation of static pressure, across the bottom liner at entry to the working section, is shown. There is encouragingly little variation evident in this case, although it must be pointed out that only about 35 per cent of the windtunnel width is covered by the data. The level of uniformity indicated is better than 0.8 per cent. This is considered satisfactory. The measured values of static pressure are used in the calculation of the boundary layer displacement thickness. The only other critical data required in this calculation are the measured pitot pressures from the rake. Thus, any non-uniformity in values of δ^* observed must be due chiefly to the variation in pitot pressure, rather than variations in static pressure.

We refer now to Figures 8 and 9. Here, the distributions of δ^* and the flow angle outside the boundary layer are shown respectively. Considering first the data obtained at the position $X = 37\text{mm}$, it is clear that there are significant variations in both δ^* and the flow angle, θ_e . The variation in δ^* is approximately 30 per cent and that in θ_e about 1.7 degree. Once again, it may be that still further variation exists beyond the range of the lateral traverse which was carried out. There is clearly a direct correlation between the forms of the lateral variation in δ^* and in θ_e at this upstream position. It is considered that a developed longitudinal vortex structure may be present, close to the bottom liner, perhaps with its core at the position $Y = 135\text{mm}$.

In Figure 9 it will be noted that all the curves drawn are broken near the windtunnel centre-line position. This break indicates the position at which data from one yawmeter ceases, and data from the other begins. As drawn, the curves indicate that there remains a small inconsistency between values of θ_e derived from the two yawmeters. This inconsistency amounts to 0.5 degree or less and is certainly much smaller than was originally feared. However, this remaining lack of agreement is still significant, so the situation is not entirely satisfactory. It could be accounted for by the presence of spanwise flow components, in which case it would improve when the spanwise

components are reduced.

Referring again to both Figure 8 and 9, it will be noted that restricted data have been presented for a third, intermediate, longitudinal position. These data are drawn from Reference 9, where a very limited investigation into windtunnel flow uniformity was reported. The flow condition involved is more severe in the sense of wall suction than in the present tests and the freestream Mach number is 0.824. There is broad agreement in the shapes of the curves for this position and those obtained at $X = 37\text{mm}$. Clearly though, being measured in the region of the perforations, the effects of considerable suction are evident. One would, on this basis, assume that the non-uniformities evident at $X = 37\text{mm}$ are swept almost directly downstream. However observation of the data obtained at $X = 240\text{mm}$, causes a re-assessment of the situation. For the boundary layer results there is good correlation between these data and those obtained at $X = 37\text{mm}$ for the blowing configuration, but little correlation for the configuration with suction through the wall. The situation is even less clear for the flow angle data. It would be difficult, in either configuration, to find correlation between the curves obtained at the two extreme longitudinal positions.

It could be stated that the non-uniformities which were evident entering the working section, are neither swept directly downstream, nor are even clearly evident downstream. It is possible that they are swept some way downstream (because they remain evident at $X = 137\text{ mm}$) into the working section, but are eventually broken up.

At an earlier stage in the investigation, it was considered that the longitudinal support webs, mounted below the perforated wall, might interfere with the process of transpiration and thus further decrease the level of uniformity evident in the windtunnel flow. The positions of three of these webs are shown in Figure 9 and one, in Figure 8. Observation of these Figures leads one to conclude that the webs do not have such an effect.

A.2.3 Implications of Results from flow uniformity investigations

It has become clear that the flow entering the working section of the windtunnel is not adequately uniform. The non-uniformities are

not swept directly downstream, but are altered and become confused as the flow passes downstream. This has implications when the experiments which have been carried out to obtain the wall-characteristic (i.e. the relation embodied in equation 2) for the perforated wall installed in the windtunnel are considered. The boundary layer and crossflow data being obtained at different lateral positions across the bottom wall, implies that in the presence of a non-uniform flow, the two sets of data are not consistent with one another. In order to obtain cross-flow data which are nearly relevant to the boundary layer rake position, it would be possible to average the values of cross-flow obtained from the two yawmeters. It appears in Figure 9 that averaging the two cross-flow values would give almost exactly the value of cross-flow which exists at the rake position. Thus, this process of re-calculation of the cross-flow characteristic should be carried out.

In future, the overall calculation method described in this research, might be used to predict

- (a) the flow of air near, and through the perforated liner in a given test; and for
- (b) the complete windtunnel flow during any particular test.

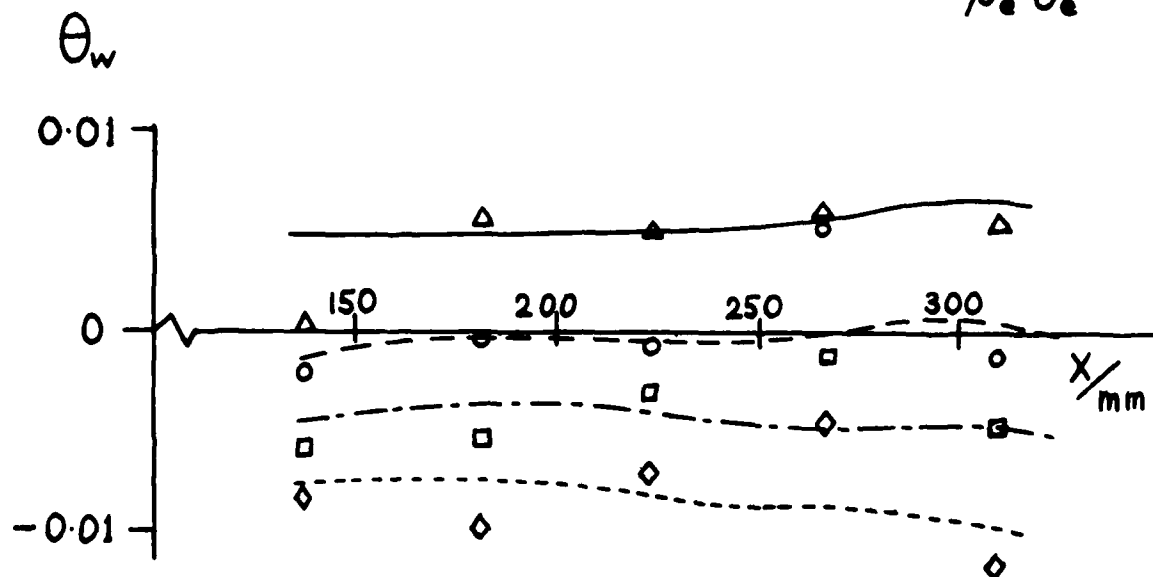
In both these applications, it would be necessary to predict the development of δ^* and θ_e along the perforated walls, with (probably) a typical aerofoil under test in the working section. In order that genuine two-dimensional developments of δ^* and θ_e exist, it will be necessary to ensure that the flow entering the working section (and developing throughout it) has adequate spanwise uniformity. Thus it would be necessary to eradicate the bulk of the variations in the quantities δ^* and θ_e , as seen in Figures 8 and 9, prior to carrying out further tests.

REFERENCES

1. R.J. Vidal, J.C. Erickson, P.A. Catlin
Experiments with a self-correcting wind tunnel.
Paper 11, AGARD CP-174, 1975.
2. D. Catherall
The computation of transonic flows past aerofoils in solid, porous or slotted windtunnels.
Paper 19, AGARD CP-174, 1975
3. B.S. Baldwin et al
Wall interference in windtunnels with slotted and porous boundaries at subsonic speeds.
NACA Technical Note 3176, 1954
4. S.B. Berndt, and H. Sorensen
Flow properties of slotted walls for transonic test sections
Paper 17, AGARD CP-174, 1975.
5. S.B. Berndt
Flow properties of slotted wall test sections.
Paper presented at AGARD meeting on Wall Interference in Windtunnels, London, May 1982.
6. Y.Y. Chan
Wall boundary layer effects in transonic wind tunnels.
Paper presented at AGARD meeting on Wall Interference in Windtunnels, London, May 1982
7. M.M. Freestone, and P. Henington
A scheme for incorporating the viscous effects of perforated windtunnel walls in two-dimensional flow calculations.
The City University Research Memo Aero 78/7, London 1979.
8. M.M. Freestone, and P. Henington
Incorporation of viscous effects of perforated windtunnel walls in two-dimensional flow calculations.
The City University Research Memo Aero 81/1, London 1981.

9. P. Henington An improved boundary condition for perforated
wall windtunnel flows.
The City University, Ph.D. Thesis, London 1982
10. M.R. Head Entrainment in the turbulent boundary layer.
Aeronautical Research Council Reports and
Memoranda No. 3152, 1960
11. Y.Y. Chan Analysis of boundary layers on perforated walls
of transonic wind tunnels
J. of Aircraft Vol.18, No.6, June 1981, pp.469-473.
12. P. Bradshaw and Design of low speed windtunnels, in
R.C. Pankhurst Progress in Aeronautical Sciences, Vol.5,
Pergamon Press, Oxford, 1963.

TRANSPIRATION PARAMETER : $\theta_w = \frac{\rho_w v_w}{\rho_e U_e}$



Flow	Observed	Predicted
1	Δ	—————
2	\circ	-----
3	\square	-.-.-.-.-
4	\diamond

FIG 1 COMPARISON OF OBSERVED AND PREDICTED
TRANSPIRATION PARAMETER VARIATIONS
FOR FOUR DIFFERENT FLOWS.

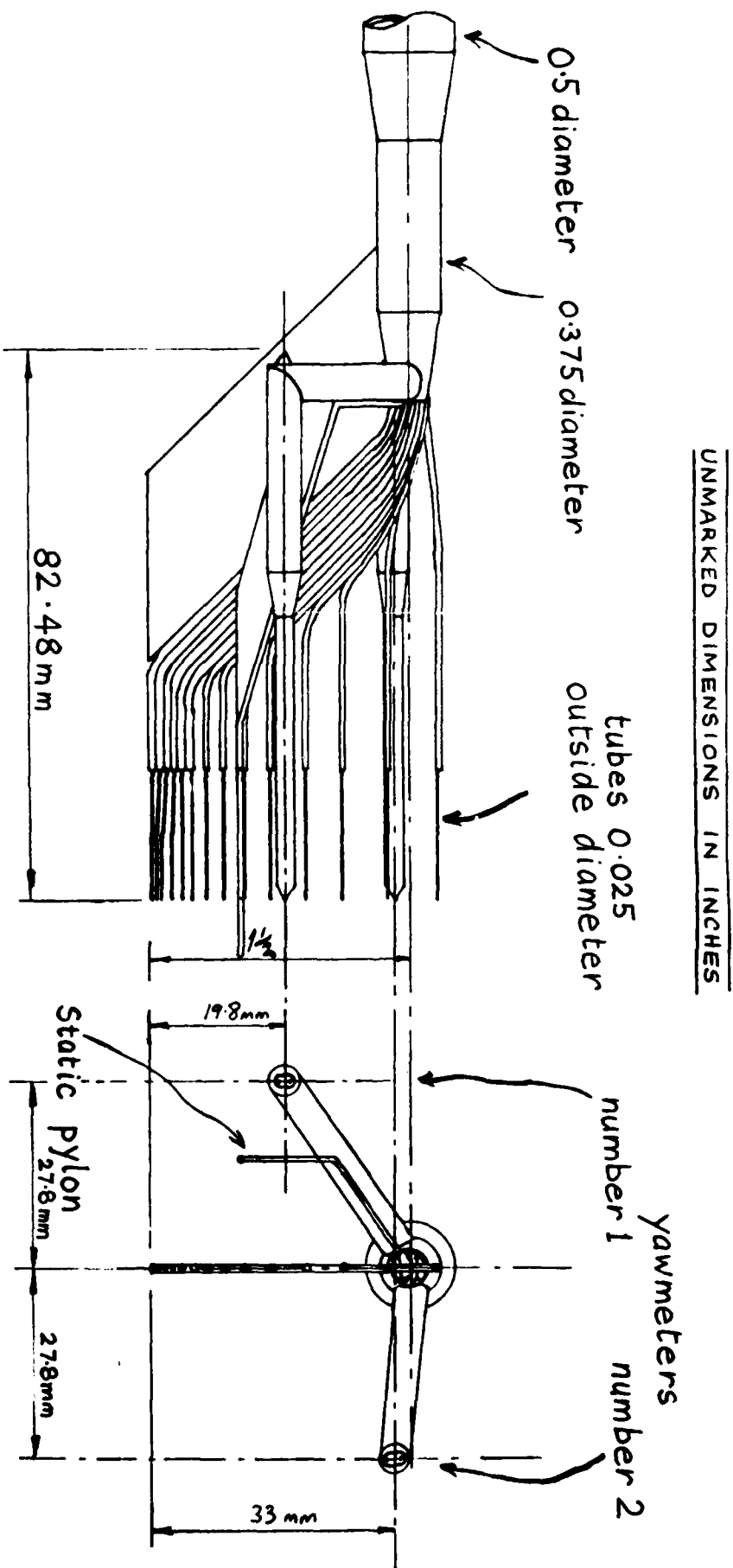


FIG2 FORWARD PART OF COMBINED BOUNDARY LAYER RAKE AND YAWMETER ASSEMBLY

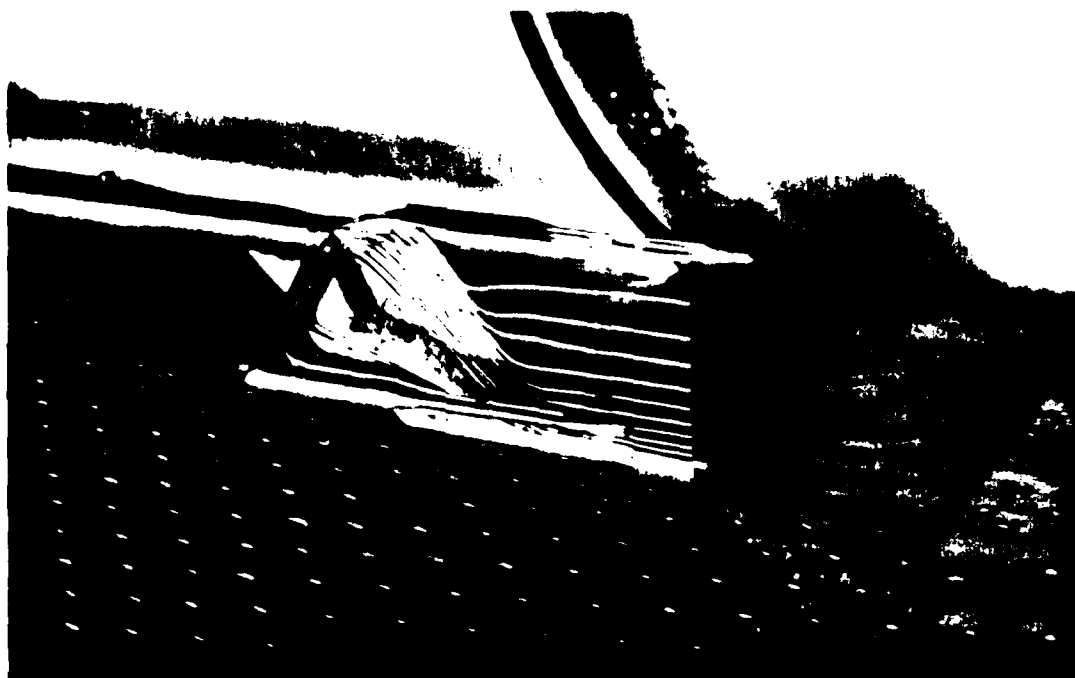


FIG3 COMBINED BOUNDARY LAYER RAKE AND
YAWMETER ASSEMBLY IN WINDTUNNEL.

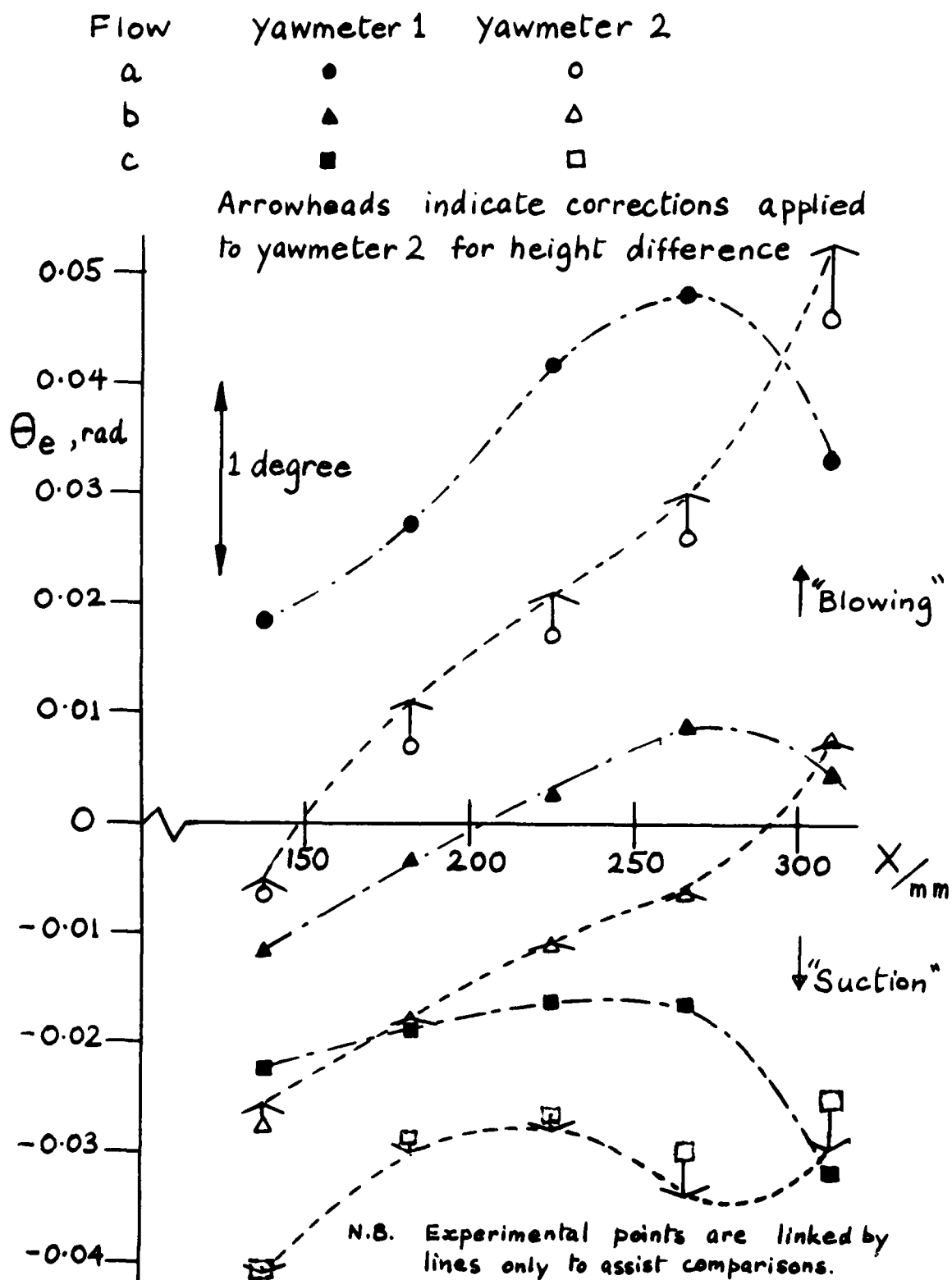


FIG 4

VARIATION OF FLOW ANGLE θ_e ALONG THE WINDTUNNEL AS GIVEN BY THE TWO YAWMETERS, FOR THREE DIFFERENT FLOWS.

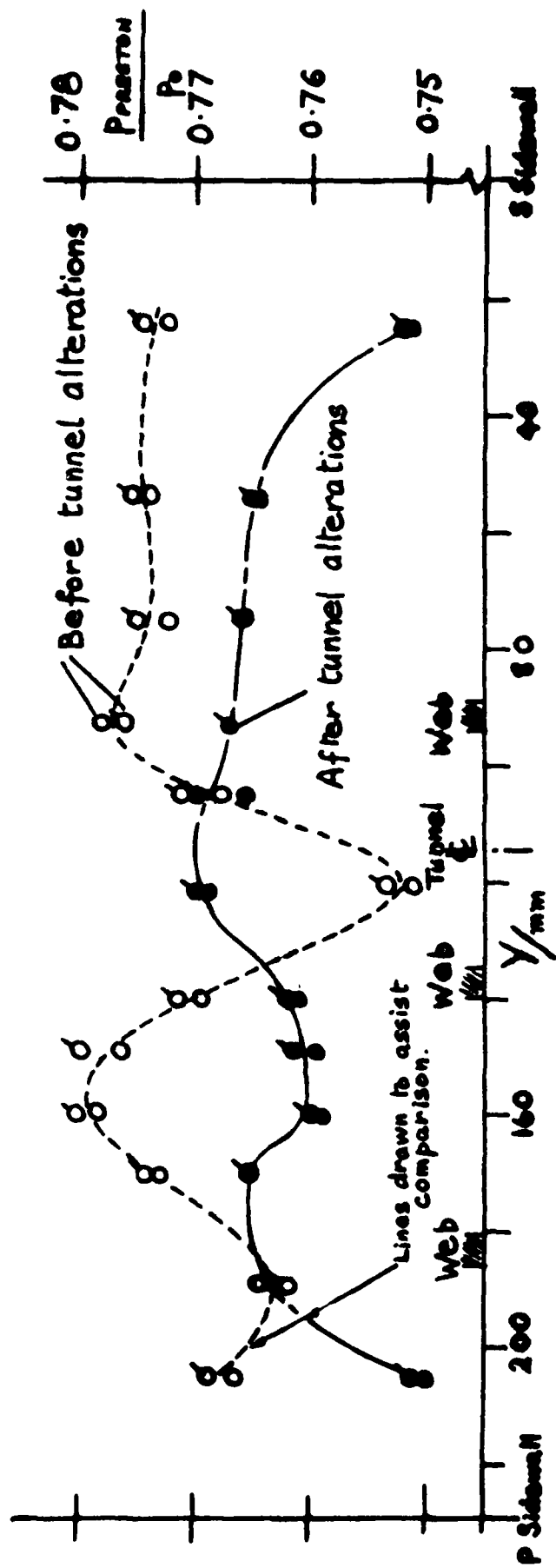


FIG 5 PRESTON TUBE PRESSURE DATA TAKEN BEFORE AND AFTER WINDTUNNEL ALTERATIONS

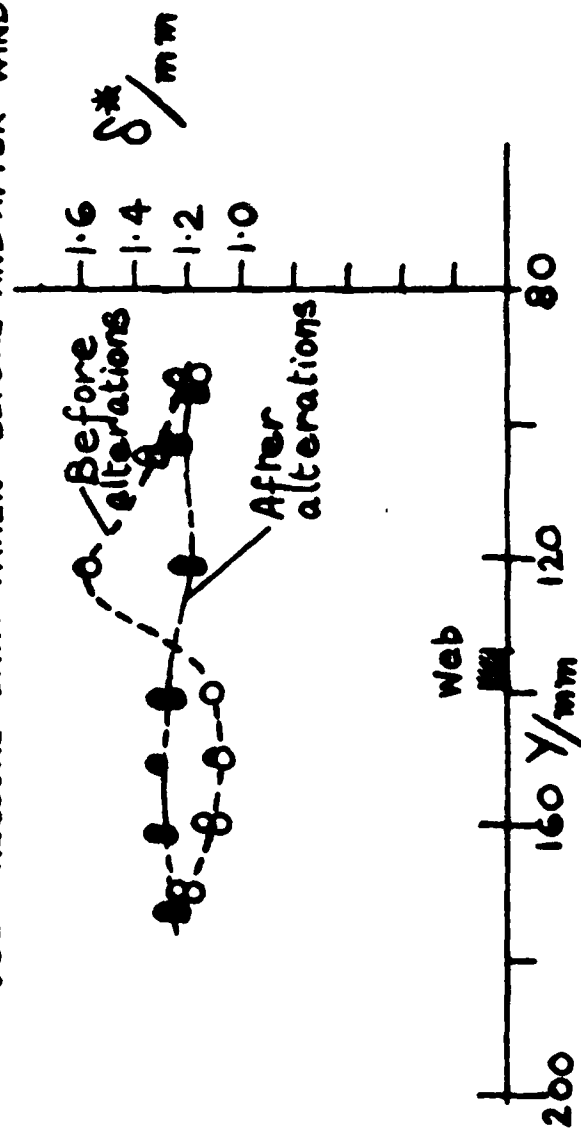


FIG 6 BOUNDARY LAYER DISPLACEMENT THICKNESS BEFORE AND AFTER WINDTUNNEL ALTERATIONS

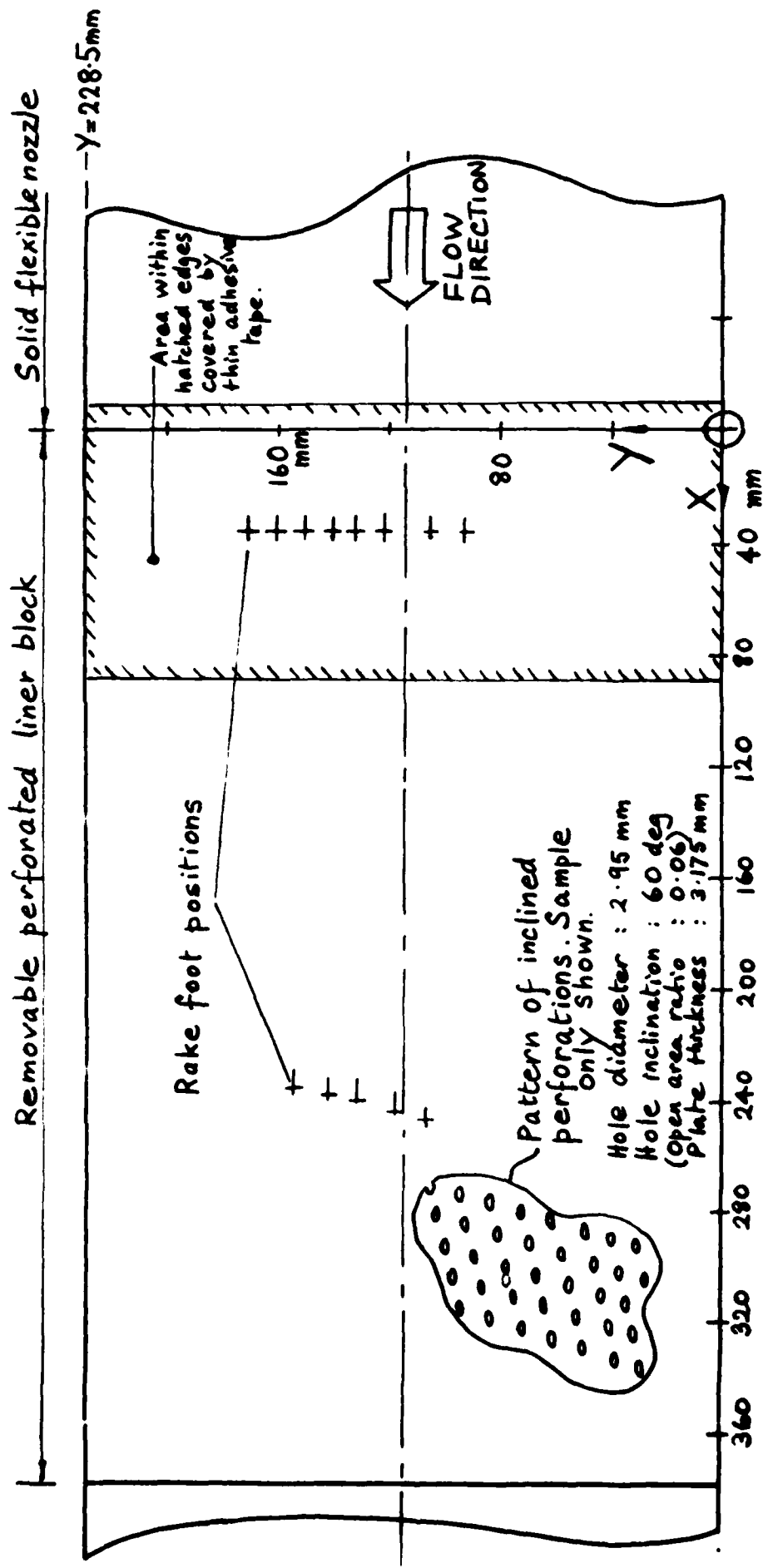


FIG 7 LAYOUT OF LOWER PERFORATED LINER OF THE CITY UNIVERSITY
TRANSONIC WINDTUNNEL
(SHOWS RAKE FOOT POSITIONS FOR FLOW UNIFORMITY INVESTIGATION)

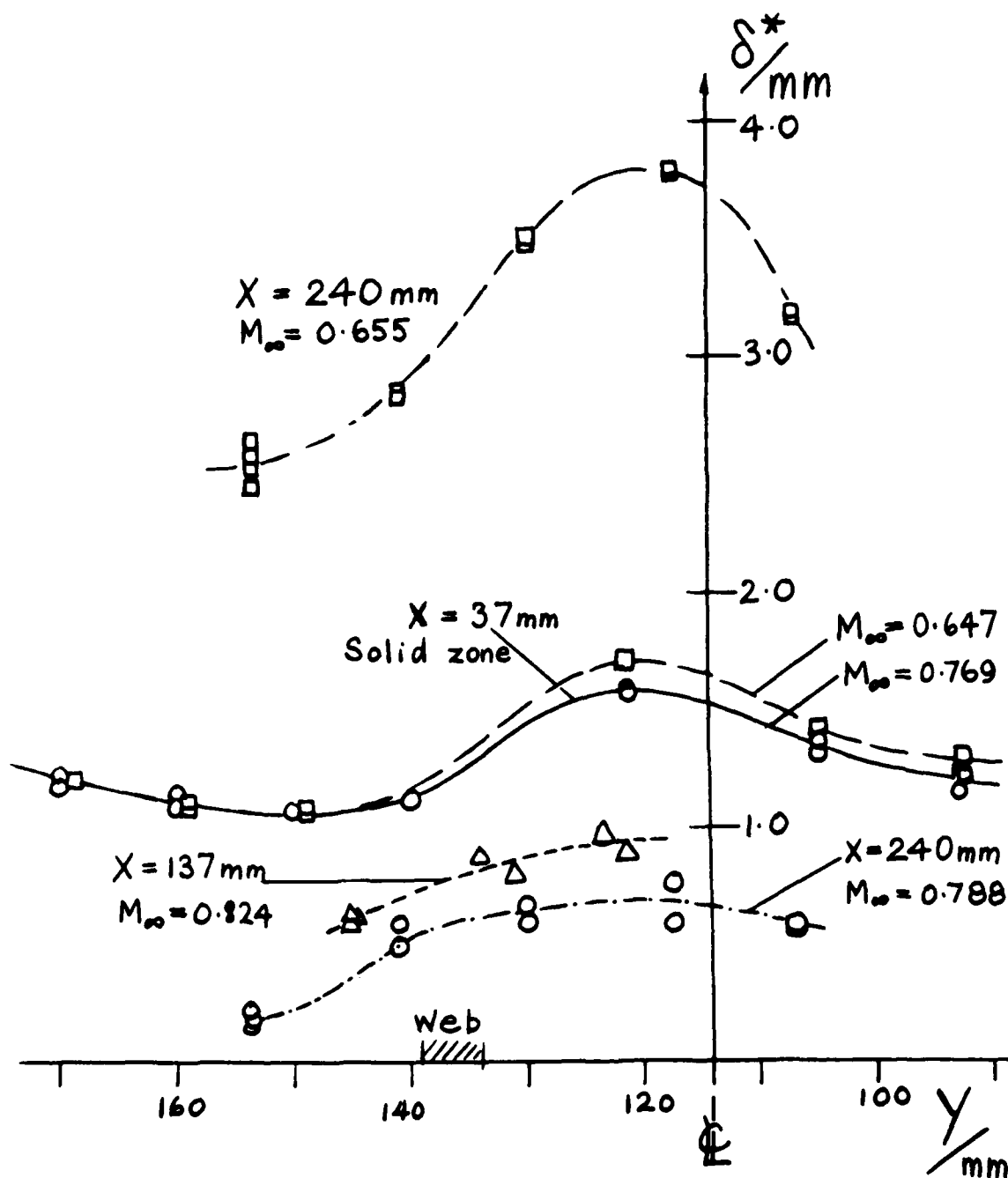


FIG 8 LATERAL VARIATIONS OF DISPLACEMENT THICKNESS ACROSS PERFORATED WALL LINER

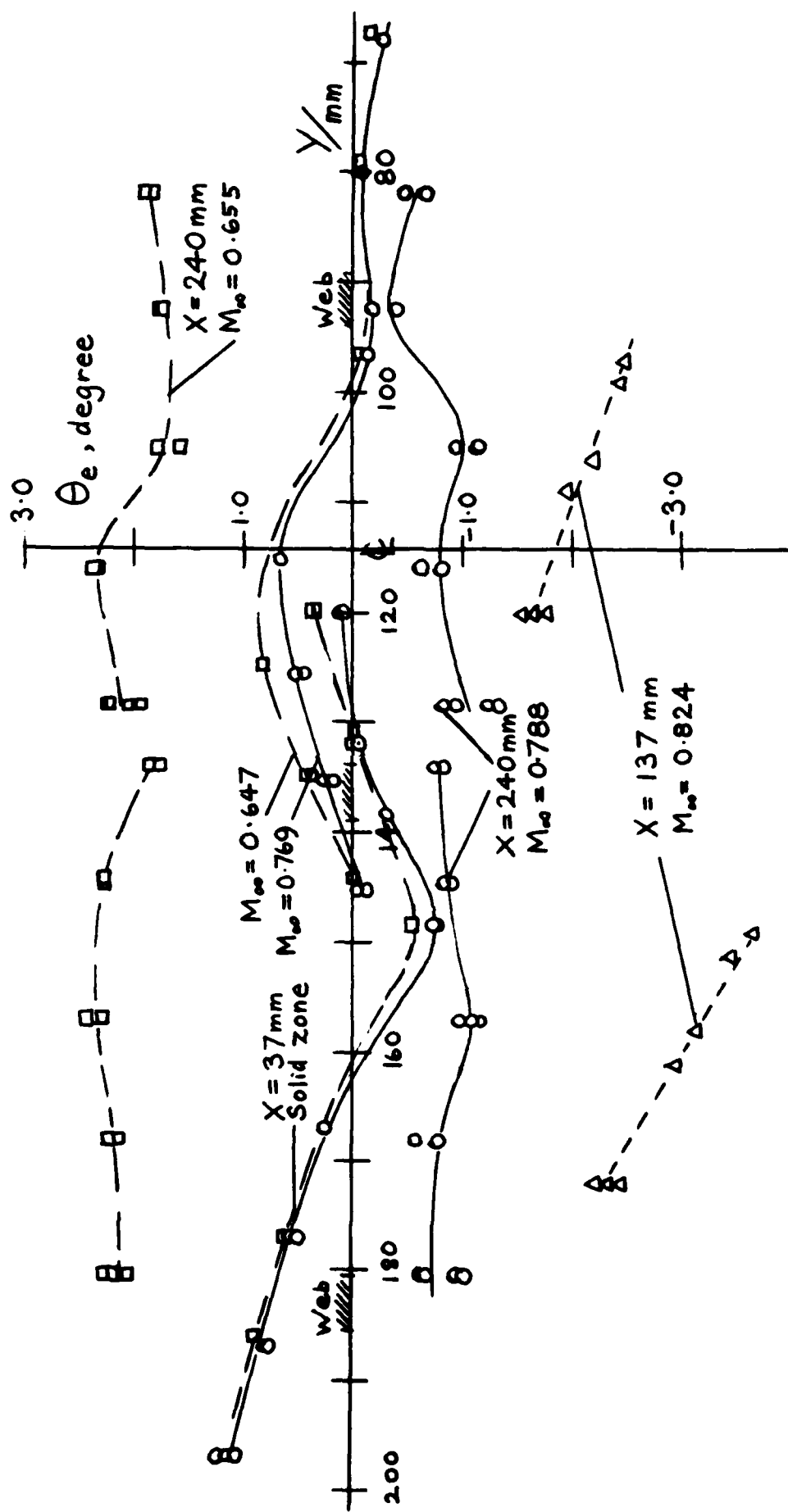


FIG 9 LATERAL VARIATIONS OF FLOW ANGLE ACROSS PERFORATED WALL LINER

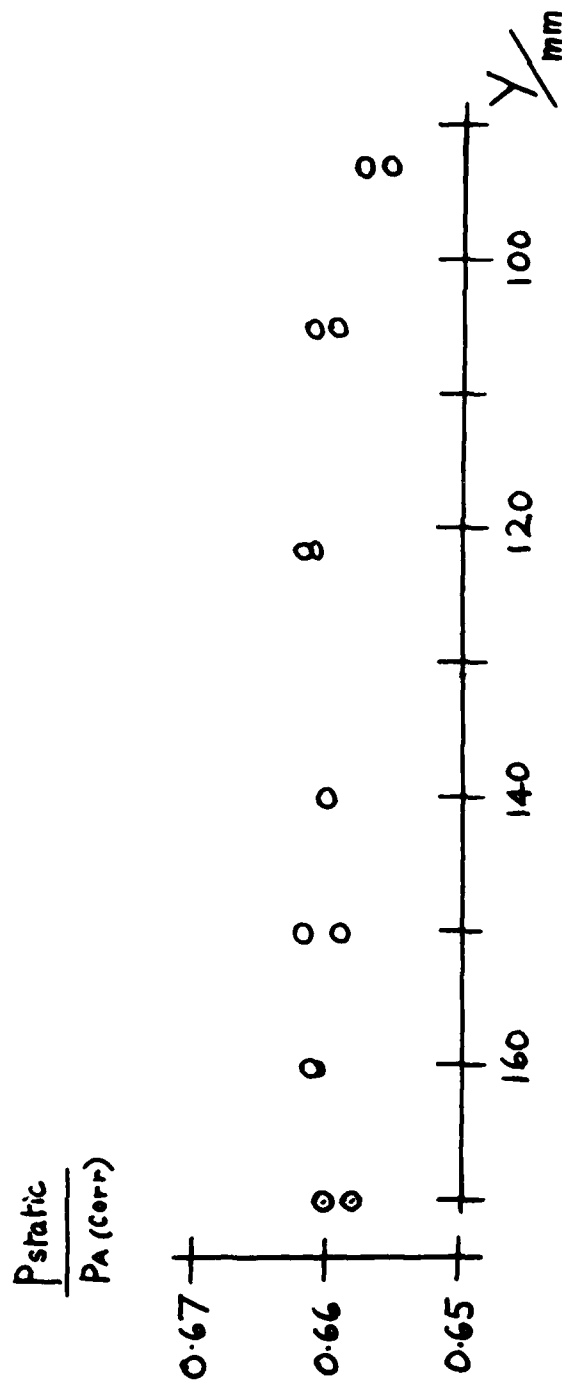


FIG 10 LATERAL VARIATION OF STATIC PRESSURE RATIO ACROSS PERFORATED WALL LINER

ATE
MED
-83